Material selection of a ferrimagnetic loaded coaxial delay line for phasing gyromagnetic nonlinear transmission lines

J. M. Johnson, D. V. Reale, W. H. Cravey, R. S. Garcia, D. H. Barnett, A. A. Neuber, J. C. Dickens, and J. J. Mankowski

Citation: Review of Scientific Instruments **86**, 084702 (2015); doi: 10.1063/1.4927719
View online: http://dx.doi.org/10.1063/1.4927719
View Table of Contents: http://aip.scitation.org/toc/rsi/86/8
Published by the American Institute of Physics

Material selection of a ferrimagnetic loaded coaxial delay line for phasing gyromagnetic nonlinear transmission lines

J. M. Johnson,[a] D. V. Reale, W. H. Cravey, R. S. Garcia, D. H. Barnett, A. A. Neuber, J. C. Dickens, and J. J. Mankowski
Department of Electrical and Computer Engineering, Center for Pulsed Power and Power Electronics, Texas Tech University, Lubbock, Texas 79409, USA

(Received 11 May 2015; accepted 21 July 2015; published online 5 August 2015)

Implementing nonlinear transmission line (NLTL) technology in the design of a high power microwave source has the benefits of producing a comparatively small and lightweight solid-state system where the emission frequency is easily tuned. Usually, smaller in physical size, single NLTLs may produce significantly less power than its vacuum based counterparts. However, combining individual NLTL outputs electrically or in free-space is an attractive solution to achieve greater output power. This paper discusses a method for aligning a four element NLTL antenna array with coaxial geometry using easily adjustable temporal delay lines. These delay lines, sometimes referred to as pulse shock lines or pulse sharpening lines, are placed serially in front of the main NLTL line. The propagation velocity in each delay line is set by the voltage amplitude of an incident pulse as well as the magnetic field bias. Each is adjustable although for the system described in this paper, the voltage is held constant while the bias is changed through applying an external DC magnetic field of varying magnitude. Three different ferrimagnetic materials are placed in the temporal delay line to evaluate which yields the greatest range of electrical delay with the least amount of variability from consecutive shots. [http://dx.doi.org/10.1063/1.4927719]

I. INTRODUCTION

A significant advantage of a nonlinear transmission line (NLTL) system as a high power microwave (HPM) source is its compact size and solid-state nature. In order to maintain the compact characteristic, a smaller megawatt class of NLTL must be used; however, there are larger gigawatt class gyromagnetic NLTLs in existence.[1] The relatively low power output from a single NLTL in this system may be increased by utilizing an array of NLTLs, and to maximize the effect of this array, the individual lines must be phased. Possible phasing methods at gigahertz regime frequencies include static electrical combination by way of a transmission line power combiner,[2] static free-space phasing using properly sized transmission lines or a type of dynamic delay. Here, dynamic delay is achieved through using a magnetically loaded transmission line where the electrical delay is manipulated by an external biasing field.[3–6] The latter option is the most versatile and space efficient making it an attractive choice in the design of a practical system; its successful implementation will be discussed in this paper.

A previous system's dynamic delay scheme used two separate biasing solenoid coils on a single NLTL. The coil towards the front of the NLTL (where the pulse enters) is smaller and magnetizes only a portion of the NLTL to control delay. The second larger coil controlled the frequency and output power of the NLTL.[3] This particular setup produced anywhere from 100 to 600 ps of adjustable delay.[2] The maximum delay of 600 ps is approximately twice a typical RF cycle for this NLTL system. Preliminary findings on the four element array, using identical main NLTLs with no delay, have shown that the four outputs can be several cycles out of phase; therefore, previous methods for output synchronization are inadequate. Dedicated delay lines, that are themselves NLTLs, are used instead to achieve greater delay times while the main NLTL remains statically biased at its optimum magnetic field level, in terms of maximum output power of the individual line, which is set by its length and ferrite characteristics. Another example of a HPM system using NLTLs, more specifically nonlinear lumped element transmission line (NLETL), to phase multiple channels is from Seddon.[7]

It is the goal of this paper to identify the ferrimagnetic material which yields the largest range of delay so that a relatively large phase offset with respect to multiple outputs may still be aligned.

For the oscillatory output of the NLTL, it is important to apply an initial magnetizing bias field to the nonlinear ferrimagnetic material, pre-aligning its magnetic moments to a partial or fully magnetized state (saturation) if the field is strong enough. As a pulse propagates through the NLTL, while sufficient external biasing is present, the magnetic moments rotate around an effective magnetic field comprised of the pulsed azimuthal field, external biasing field, demagnetizing fields, exchange fields, and anisotropy fields where $\mathbf{H}_{eff}$ denotes the time and spatially varying effective magnetic field. This rotational process is known as gyromagnetic precession. More specifically, it is damped gyromagnetic precession since the magnetic domains realign, or relax, with $\mathbf{H}_{eff}$

[a]Electronic mail: jared.johnson@ttu.edu

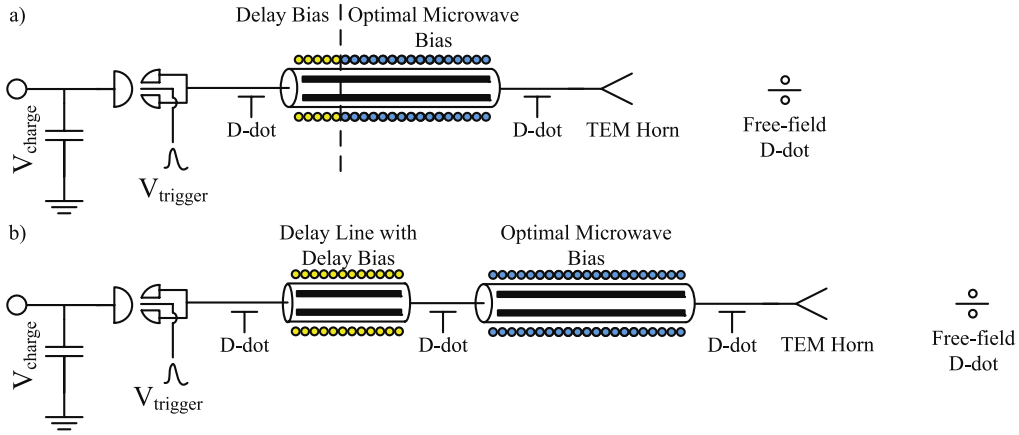

FIG. 1. (a) Schematic of NLTL system using two separate coils on a single line for the purpose of electrical delay and phase alignment and (b) schematic of tandem NLTL system using two individual NLTLs connected serially for pulse delay.

once the pulse has ended. This process is described by the Landau-Lifshitz equation,

$$\frac{\partial \mathbf{M}}{\partial t} = \gamma(\mathbf{M} \times \mathbf{H}_{eff}) - \frac{\alpha}{M_s}(\mathbf{M} \times (\mathbf{M} \times \mathbf{H}_{eff})), \quad (1)$$

where the first term describes the precession of the magnetic moments around the effective magnetic field and the second term describes the damping action which eventually ends the precession and relaxes the magnetic moments back to $\mathbf{H}_{eff}$. γ represents the gyromagnetic ratio which is equal to -2.21 (s A/m)$^{-1}$, M_s is the magnetization at saturation and α represents the damping term which is not fully understood and is considered an empirical quantity.[8]

There is no difference between the main NLTL and the dedicated delay line other than length and applied bias. One is biased for optimum microwave power output and the other is biased for delay. Equation (1) is valid for both lines. The longer the ferrimagnetic loaded line that is biased at a single bias level, the greater potential there is for delay. Simply put, this is because there is a greater distance for a wave to traverse with a varying propagation velocity due to a varying μ set by the user. Equation (2) is the expression for wave propagation velocity where one can see the dependence of the velocity on μ.

$$v = \frac{c}{\sqrt{\epsilon_r \mu_r}}. \quad (2)$$

More information on the mechanisms of pulse sharpening, shock front formation, and damped gyromagnetic precession can be found here.[9–13]

II. EXPERIMENTAL SETUP

Figure 1 illustrates a schematic of the NLTL system. The NLTL is excited by a discharge pulse from a 5.2 nF capacitor bank that is charged to −40 kV. The high power switch is a trigatron spark gap filled with pressurized dry air, and this switch is closed by a pulse trigger generator. Details about the design and performance characteristics of the trigger generator may be found elsewhere.[14] Briefly, the peak voltage of the trigger pulse is selected to be half of the charge voltage (20 kV), and since the main charge is of a negative polarity, the trigger pulse has a positive polarity for maximum field enhancement as well as positive streamer formation. Negative charging and positive triggering is the fastest configuration for breakdown in a center electrode trigatron spark gap.[15] Switching times for the spark gap are around ∼7 ns 10%-90%. Pressurized sulfur hexafluoride (SF_6) is the insulator between the inner and outer conductor throughout the NLTL complimented by Kapton® tubing with wall thickness of 264 μm fitted over the ferrites.

The delay lines are serially placed in between the pulse source and the main NLTLs. The three materials tested are all NiZn ferrites: material 43, 61, and NiZn1. Materials 43 and 61 are manufactured by Fair-Rite and NiZn1 by Metamagnetics, see Table I for a summary of the ferrites' characteristics. Specifically, NiZn1 is used as the ferrimagnetic material in the main NLTL due to its superior microwave output performance at −40 kV charging. The biasing field generated by the solenoid coil for the NLTL remains at 20 kA/m since microwave output was at its highest for that field strength with

TABLE I. Summary of ferrimagnetic materials. Omitted information for NiZn1 is proprietary.

	Initial permeability μ_i	B (G) at H (Oe)	Residual B_r (G)	Coercive H_c (Oe)	Loss factor $\tan(\delta/\mu_i)$ at 1 MHz	Curie temperature T_c (°C)	Resistivity ρ (Ω-cm)
M43	800	2900 at 10	1300	0.45	2.5×10^{-4}	>130	1×10^5
M61	125	2350 at 15	1200	1.8	3.0×10^{-5}	>300	1×10^8
NiZn1	NiZn1(μ_i) > M43(μ_i) > M61(μ_i)					$\epsilon_r = 15$	

the given line geometry and ferrite.[16] For more information on NiZn1, see Ref. 10. Here, NiZn1 and "MX7"are the same ferrite material.

Two basic methods of temporally aligning the pulse output of NLTLs are depicted in Figure 1. While the integrated delay and microwave NLTL approach, see Figure 1(a), had limited success, the tandem NLTL, see Figure 1(b), has overcome these limits. In the tandem approach, the method presently explored, a dedicated delay line is implemented instead of only biasing the front portion of the main NLTL. The three custom-made, "in-line" D-dot probes in Figure 1(b) are utilized to measure the voltage waveforms before and after the delay line and NLTL. A fourth D-dot, Prodyn Technologies' AD-70 with a 3 dB point of 3.5 GHz and sensitivity up to 11 ps 10%-90% rise time is used to measure free-space field emissions. Voltage signals are attenuated by approximately 100 dB before being sampled by a 50 GHz, 160 Gsa/s digital oscilloscope made by Keysight Technologies.

The NLTL is terminated into a custom made TEM horn antenna with Rexolite® as the dielectric. The coaxial geometry of the NLTL is transformed to a parallel configuration via a zipper balun, also using Rexolite, to feed the antenna. A zipper balun gradually transitions from an enclosed coaxial transmission line (unbalanced) to an open parallel plate configuration (balanced) which is ideal for TEM horn input. When looked upon, this balun resembles an "un-zipped" zipper thus explaining its name and remarkable tapered characteristic. Because the transition is gradual, the impedance change is small per unit length of the balun; therefore, reflections are small allowing for maximum transmitted power. Also, the balun must be long enough to achieve a balanced parallel plate output.

III. RESULTS

The method or standard for measuring delay in this experiment is defined as the difference of time for the initial pulse to reach a set voltage difference during its fall time (t_0) and the time it takes for the NLTL output oscillation to reach its first zero crossing (t_1). Figures 2 and 3 illustrate this. First, the initial pulse is integrated to show the true voltage waveform since it is measured with a D-dot probe. Any DC offset is removed before the integration, and then the time it takes to satisfy a constant voltage difference is recorded as t_0. The output waveform in Figure 3 is left in its raw derivative form. The first zero crossing during the oscillation is measured and recorded as t_1. Now, t_0 is subtracted from t_1.

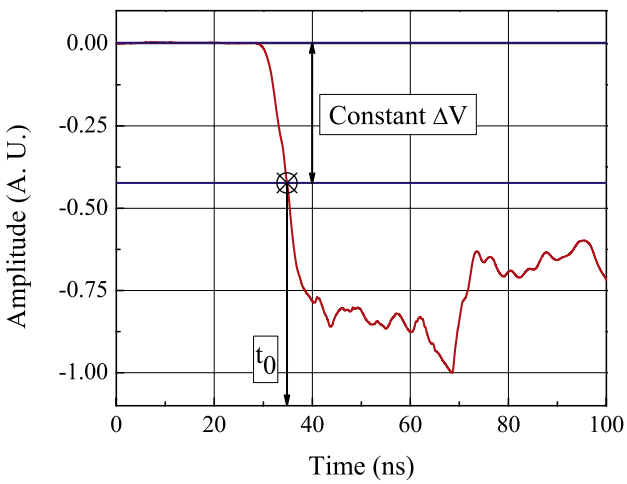

FIG. 2. Time delay measurement at constant ΔV crossing of the falling edge on the integrated and normalized incident pulse with DC offset removed. Measurement taken with the first "in-line" D-dot probe from Figure 1(b).

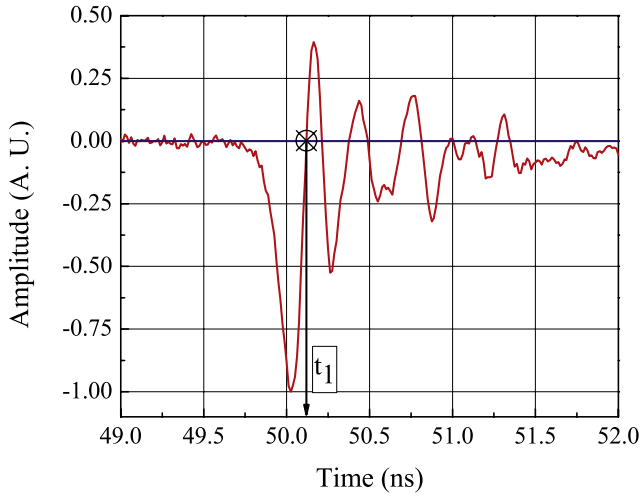

FIG. 3. Normalized raw derivative signal of the NLTL output measured using the third "in-line" D-dot probe from Figure 1(b). Time measurement at zero crossing.

This process is performed over a range of magnetic field biases (0-25 kA/m, step of 1 kA/m) applied to the delay line while the NLTL's bias remains constant. At each bias point, 10 shots are taken for statistical analysis of the repeatability and consistency of the delay times measured. All of these actions listed here and above are executed through an automated Matlab script.

Figure 4 shows the time difference of t_0 from t_1 as

$$\Delta t = t_1 - t_0 \tag{3}$$

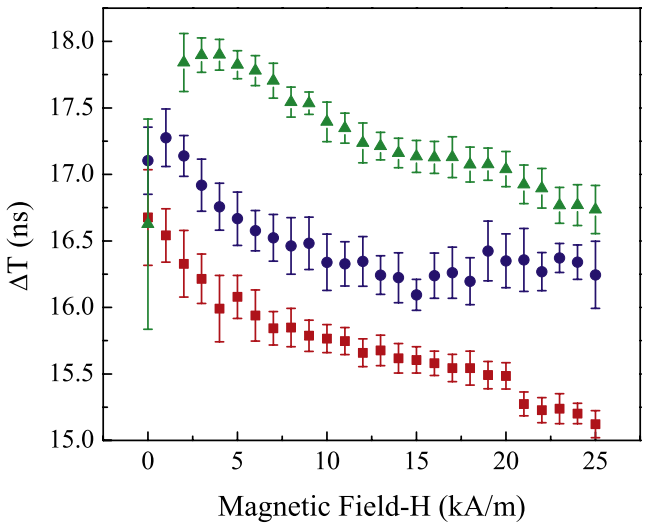

FIG. 4. Delay time vs. magnetic field bias where NiZn1 (□), M43 (○), and M61 (△). This graph shows a 10 shot average delay time with associated error bars (representing standard deviation) at a given magnetic field bias for each material.

with the corresponding magnetic bias field. Each point represents a 10 shot average of delay time, and each error bar represents a 10 shot average of the associated standard deviation. Also, each color and corresponding shape show the performance of a different material. To better show the repeatability, or lack thereof, from consecutive shots, Figure 5 is presented. This graph plots the ratio of average time delay from 10 consecutive shots per standard deviation of the same 10 shots. The greater the ratio, the more consistent each shot is to the others and vice versa.

All materials show a general trend of decreasing delay time as the magnetic field bias is increased. The range of variability for each material (max to min Y axis value), which is the maximum possible delay for a given material, is NiZn1: 1.56 ns, M43: 1.19 ns and M61: 1.16 ns. Another trend, the NiZn1 material becomes more consistent from shot to shot as the bias field is increased; whereas, the other two materials' consistency is not as noticeably effected by the bias level. Additionally, the average of the standard deviation for each output peak from Fig. 3 at a single bias setting for each material is calculated due to its significant effect on delay standard deviation. They are as follows, NiZn1: 3.9%, M43: 4.4%, and M61: 4.0%. Also, the stability of the current supply at any given setting in the form of tolerance is less than 0.25%, or the approximate equivalent of 2.5 A/m.

Figure 6 shows two independent radiated waveforms output from all four NLTLs from the same source. Once the trigatron spark gap switch closes, the current is split four ways by a symmetrical distribution plate that is connected to the adjacent electrode feeding each NLTL. When the delay measurements were made, only one line was used, and the other three outputs were left open. The radiated waveforms from the individual NLTLs combine in free space and are measured using a free-field sensing D-dot probe. These signals are left unintegrated, and the waveforms are normalized to demonstrate phasing by shape rather than voltage and power increase.

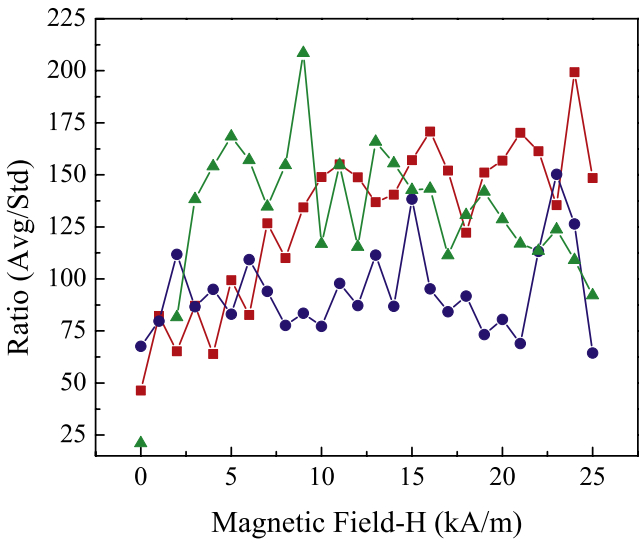

FIG. 5. Ratio of average delay time to corresponding standard deviation vs. magnetic field bias level comparing all three materials where NiZn1 (□), M43 (○), and M61 (△).

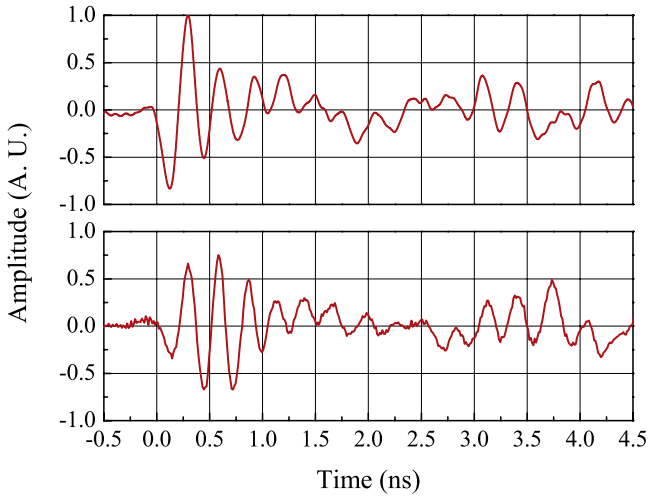

FIG. 6. Radiated NLTL outputs juxtaposed with phasing, top, and without, bottom. Both waveforms are normalized to the positive peak of the phased waveform and both were measured with the fourth D-dot probe for free-field measurements from Figure 1(b) using the same amount of attenuation. The waveform without phasing has all NLTLs and delay lines biased to a single, optimal bias field for microwave production.

The peak of the NLTL microwave is at its greatest on the second oscillation so radiated signals that are properly phased should have this same characteristic. One can see in Figure 6 that from 0 to 1.5 ns the envelope of the microwave with good phasing has this trait, while the other does not. The envelope without phasing resembles a gaussian shape, as opposed to a more nearly exponential envelope when proper phasing is applied. This is not to say that when no delay for phasing is applied that the combined output should have a Gaussian envelope; it is merely a coincidence. It is interesting to note that the waveform without phasing has all bias values for each delay line and NLTL set to the optimal value for microwave production. With all biases set the same, the system should be perfectly in phase; however, in reality, this is not the case.

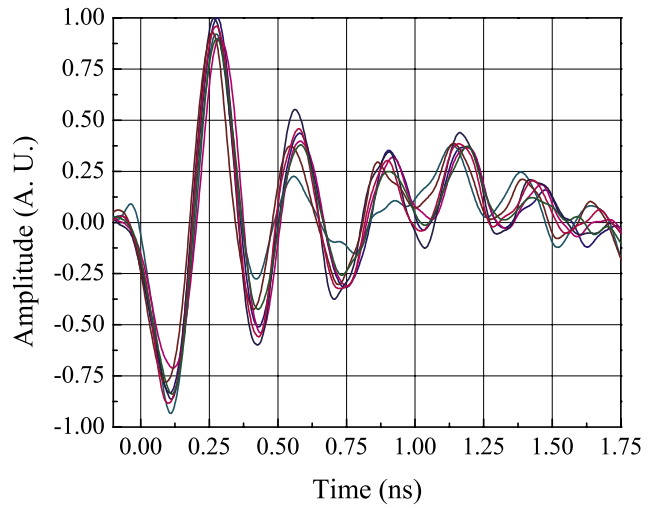

FIG. 7. Seven consecutive shots overlayed that are radiated from a phased 4 element antenna array. Waveforms were measured using the fourth D-dot probe for free-field measurements from Figure 1(b).

One may also note in Figure 6, demonstrating proper phasing, that reflections several cycles out from 3 to 4 ns are on the order of the peak amplitude of the waveform without phasing. This is not so when proper phasing is implemented. Figure 7 illustrates the repeatability of the NLTL system while phased. Seven consecutive normalized shots are overlayed and reasonably good consistency from shot to shot can be observed. As with Figure 6, these 7 signals are left unintegrated and were measured using the same probe.

IV. CONCLUSION

Based on the analysis of the data, it is clear that the NiZn1 ferrimagnetic material is optimal for achieving maximum phase delay. Though all materials show a large improvement in electrical delay performance using dedicated delay lines, NiZn1 has the greatest range of possible delay. This delay is almost triple compared to a previous maximum of 600 ps. The superior delay range is complimented by also having the lowest average standard deviation per bias setting.

The primary reason for the improved electrical delay range by using 2 NLTLs in series is based on the length of the transmission line that is biased differently. Previously, only a small portion of the NLTL could be biased differently, and thus its delay range was limited. Another possible solution is to simply lengthen the delay coil from Figure 1(a). However, maintaining the present configuration is preferred since it produces the greatest amount of power, also using the NiZn1 material, which was previously recorded. Therefore, adding a dedicated delay NLTL in series with the main NLTL is the most versatile and compact solution for phasing purposes on the described system.

Future work includes operating the synchronized NLTL array at high repetition rates for maximum average power at a far-field point and biasing the dedicated delay lines for the purpose of beam steering the 4 element antenna array.

ACKNOWLEDGMENTS

This work is supported by the Office of Naval Research.

[1]I. V. Romanchenko, V. V. Rostov, A. I. Klimov, I. K. Kurkan, A. V. Gunin, V. I. Koshelev, K. N. Sukhushin, Y. A. Andreev, and V. Y. Konev, "Effective irradiation of high-power RF pulses from gyromagnetic nonlinear transmission lines," in *2013 19th IEEE Pulsed Power Conference (PPC)* (IEEE, 2013), pp. 1–5.

[2]D. Reale, J.-W. Bragg, N. Gonsalves, J. Johnson, A. Neuber, J. Dickens, and J. Mankowski, "Bias-field controlled phasing and power combination of gyromagnetic nonlinear transmission lines," Rev. Sci. Instrum. **85**, 054706 (2014).

[3]J. Bragg, C. Simmons, J. C. Dickens, and A. A. Neuber, "Serial arrangement of ferrimagnetic nonlinear transmission lines," in *2012 IEEE International Power Modulator and High Voltage Conference (IPMHVC)* (IEEE, 2012), pp. 229–230.

[4]V. Rostov, A. Elchaninov, I. Romanchenko, and M. Yalandin, "A coherent two-channel source of Cherenkov superradiance pulses," Appl. Phys. Lett. **100**, 224102 (2012).

[5]V. V. Rostov, A. A. El'chaninov, A. I. Klimov, V. Y. Konev, I. V. Romanchenko, K. A. Sharypov, S. A. Shunailov, M. R. Ul'maskulov, and M. I. Yalandin, "Phase control in parallel channels of shock-excited microwave nanosecond oscillators," IEEE Trans. Plasma Sci. **41**, 2735–2741 (2013).

[6]I. Romanchenko, V. Rostov, A. Gunin, and V. Y. Konev, "High power microwave beam steering based on gyromagnetic nonlinear transmission lines," J. Appl. Phys. **117**, 214907 (2015).

[7]N. Seddon, C. Spikings, and J. Dolan, "RF pulse formation in nonlinear transmission lines," in *2007 16th IEEE International Pulsed Power Conference* (IEEE, 2007), Vol. 1, pp. 678–681.

[8]J.-W. B. Bragg, "Ferrimagnetic-based, coaxial nonlinear transmission lines," Ph.D. thesis, Texas Tech University, 2012.

[9]J. Dolan and H. Bolton, "Shock front development in ferrite-loaded coaxial lines with axial bias," in *IEE Proceedings–Science, Measurement and Technology* (IET, 2000), Vol. 147, pp. 237–242.

[10]J.-W. Bragg, J. Dickens, and A. Neuber, "Material selection considerations for coaxial, ferrimagnetic-based nonlinear transmission lines," J. Appl. Phys. **113**, 064904 (2013).

[11]M. Weiner and L. Silber, "Pulse sharpening effects in ferrites," IEEE Trans. Magn. **17**, 1472–1477 (1981).

[12]T. Benson, R. Pouladian-Kari, and A. Shapland, "Novel operation of ferrite loaded coaxial lines for pulse sharpening applications," Electron. Lett. **27**, 861–863 (1991).

[13]J. Dolan and H. Bolton, "Length equation for ferrite-loaded high voltage pulse sharpening lines," Electron. Lett. **34**, 1299–1300 (1998).

[14]D. H. Barnett, J. M. Parson, C. F. Lynn, P. M. Kelly, M. Taylor, S. Calico, M. C. Scott, J. C. Dickens, A. A. Neuber, and J. J. Mankowski, "Optically isolated, 2 kHz repetition rate, 4 kV solid-state pulse trigger generator," Rev. Sci. Instrum. **86**, 034702 (2015).

[15]S. J. MacGregor, F. Tuema, S. Turnbull, and O. Farish, "The influence of polarity on trigatron switching performance," IEEE Trans. Plasma Sci. **25**, 118–123 (1997).

[16]D. V. Reale, "Coaxial ferrimagnetic based gyromagnetic nonlinear transmission lines as compact high power microwave sources," Ph.D. thesis, Texas Tech University, 2013.